

Lecture 30

- Solar Wind: Stix pp. 403-412,
- Knipp, pp. 200-207

Last time...

- How to take limits
- Partial derivatives commute
- Wave trains
- Working with Kronecker deltas
- Chromosphere
- Corona
- Solar Wind

Titan's Anti-greenhouse Effect

Where does it come from, how does it work,
and how much does it cool the surface?

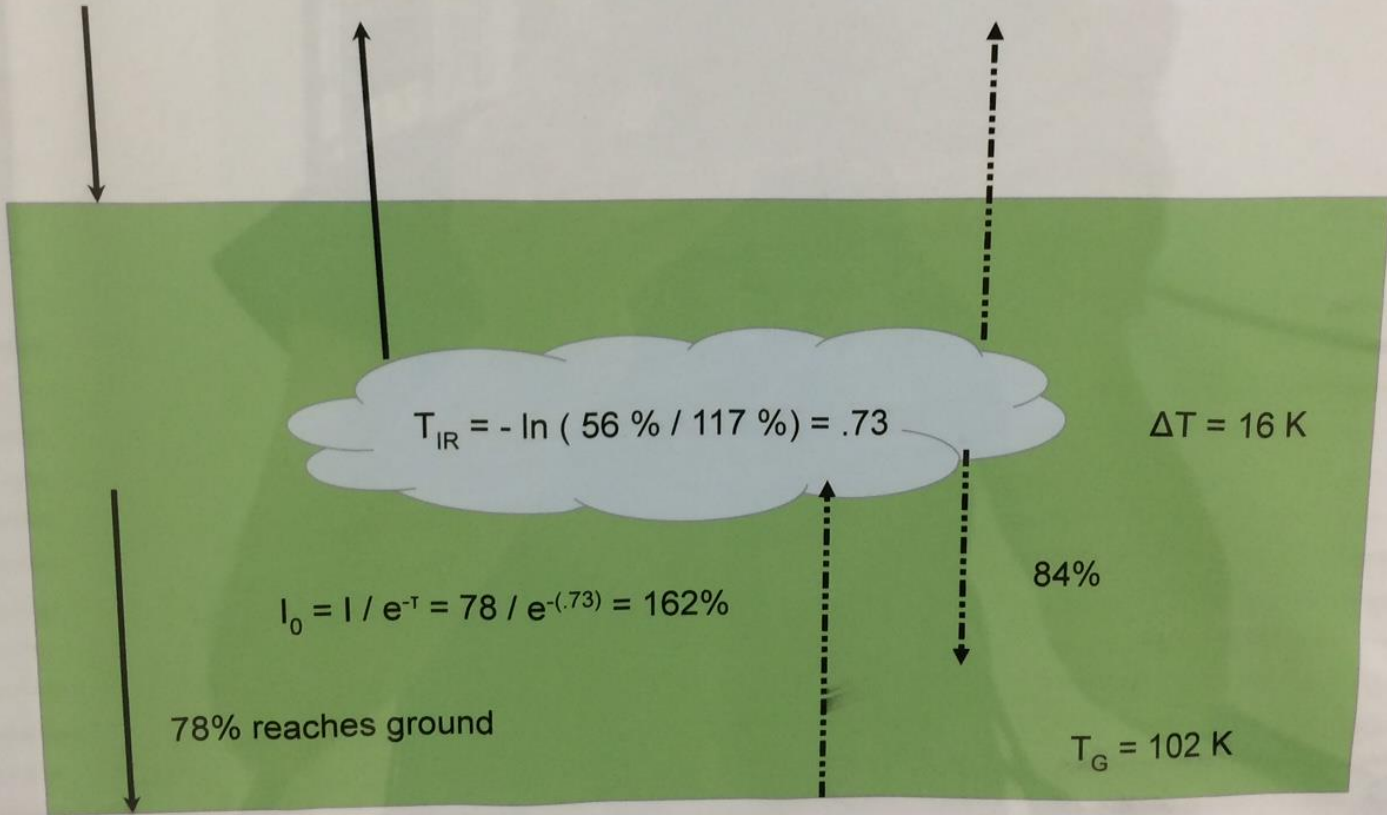
Ben Levin, Kate Wachs, Damien Burks

No Haze Layer

100 % = 3.77 W / m²

22% reflected

78% = 2.94 W / m² = 85 K



$$T_{IR} = -\ln(56\% / 117\%) = .73$$

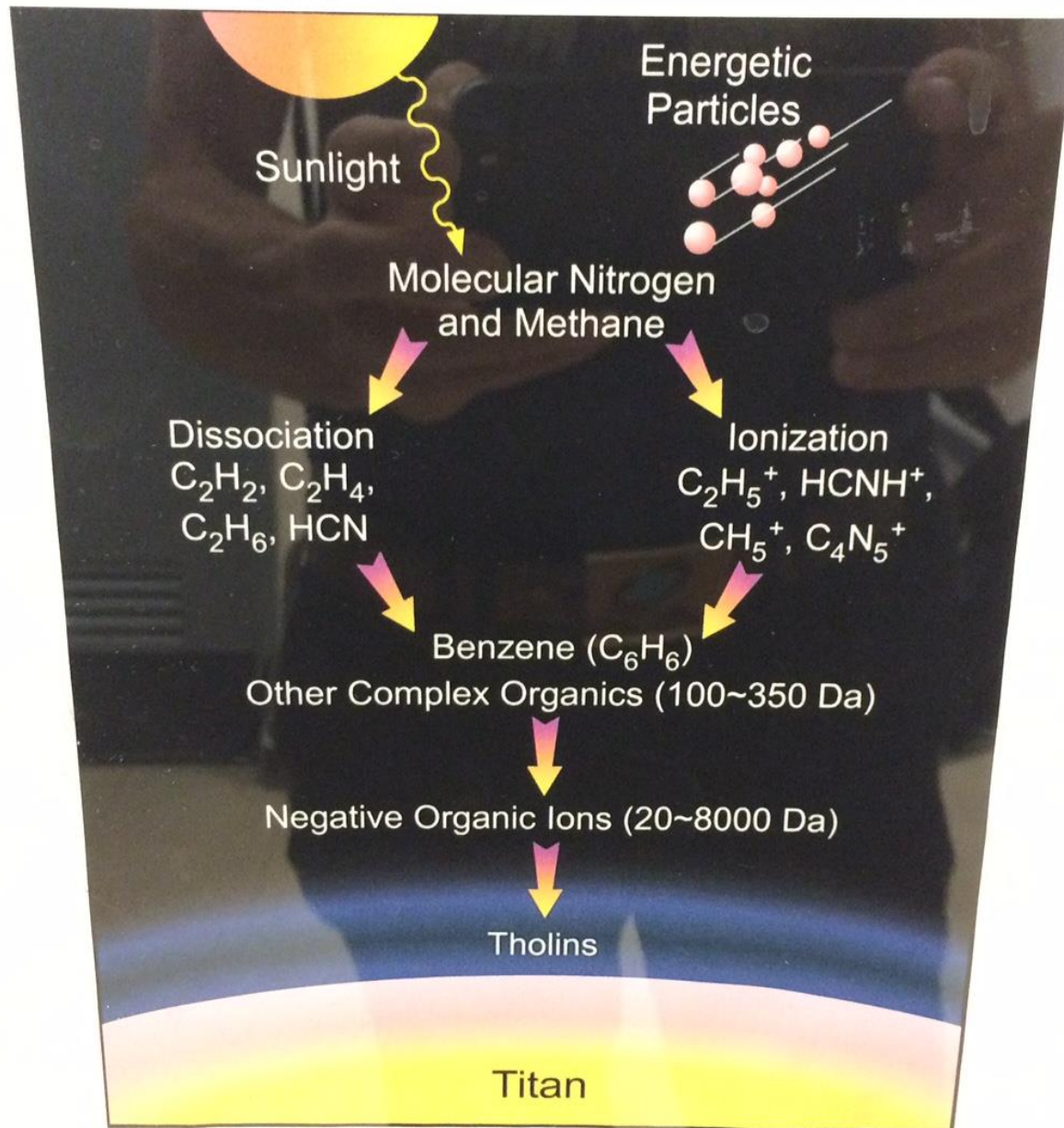
ΔT = 16 K

$$I_0 = I / e^{-\tau} = 78 / e^{-(.73)} = 162\%$$

84%

78% reaches ground

T_G = 102 K



Conclusions

Greenhouse effect: + 16 K

Anti-greenhouse effect: - 7 K

Net greenhouse effect: + 9 K

We determined that the greenhouse effect of Titan is offset by an anti-greenhouse effect, causing a net increase of temperature around 9 K. This agrees (to a reasonable degree) with the published numbers of McKay et. al (1991) of

Greenhouse effect: + 21 K

Anti-greenhouse effect: - 9 K

Net greenhouse effect: + 12 K

Considering their inclusions of multiple other factors within the energy balance and their use of 82 K as T_{eff} and 0.30 instead of 0.22 as the albedo. They considered the effects of convective flux and ground-level reflectivity, which we omitted. In both instances, it was calculated that the anti-greenhouse effect is roughly half of the greenhouse effect.

We also determined how much the atmosphere would be heated if the haze layer were not present. In that case, the surface temperature would be 102 K, which is much greater than the actual temperature of 94 K.

Cooling effects happen elsewhere in the solar system. On Pluto, instead of heating the surface, solar radiation sublimates nitrogen ice. This acts as a cooling mechanism but is not a true anti-greenhouse effect. Knowledge of anti-greenhouse effects has challenged beliefs about the early Earth and its heating mechanisms as well.

Future works could include direct calculation of the optical depths and absorption cross sectional area of different wavelengths for the particular composition of the haze. A more comprehensive collection of the Huygens data could be used to better calculate results. Also useful would be a probe that started taking measurements at the haze layer instead of far below it.

Halpna:

Large-scale
network



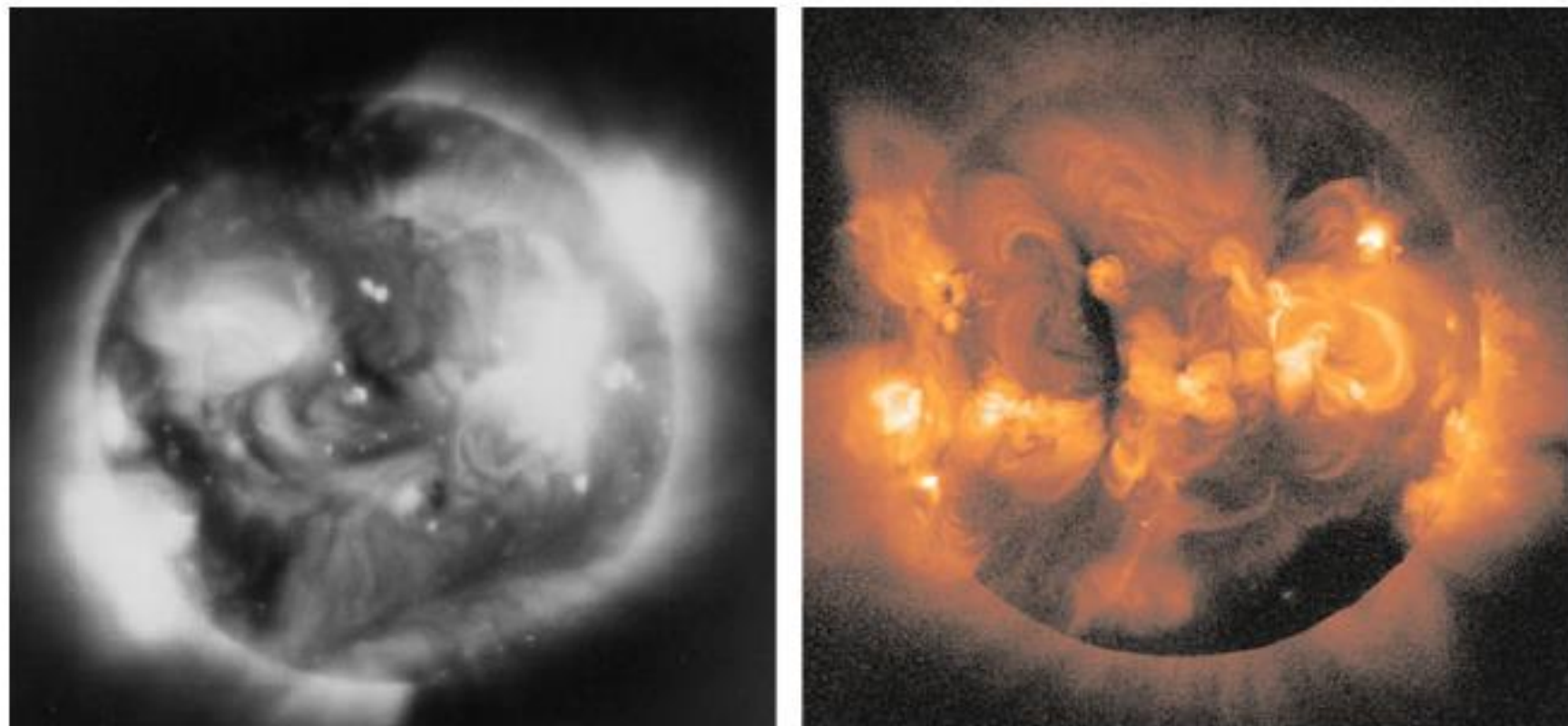


Fig. 9.10. Images of the Sun in soft x-rays (0.3–6 nm), obtained in 1973 by the Skylab mission (*left*, Vaiana et al. 1973), and in 1991 by Yohkoh (*right*)

Inspection of a coronal x-ray image immediately suggests that we must distinguish between two types of coronal regions: bright and dark. The bright

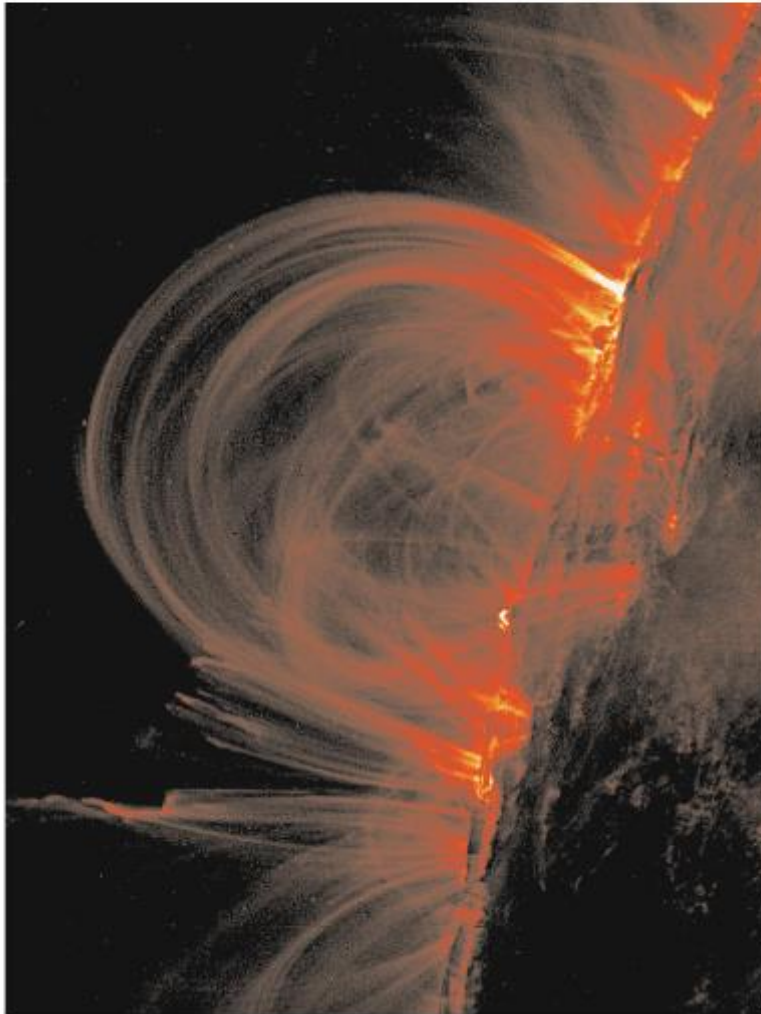


Fig. 9.9. Coronal loops at the solar limb, seen in the 17.1-nm pass band by the normal-incidence telescope on the satellite TRACE. The image (exposure 19.5 s) was taken on 6 November 1999; it shows plasma of $\approx 10^6$ K and has been evaluated by Aschwanden et al. (2000, 2001). Courtesy C. J. Schrijver

Figure 9.9 is a TRACE image that shows plasma loops in a spectral band of width ≈ 0.6 nm around 17.1 nm, containing emission lines of Fe IV and

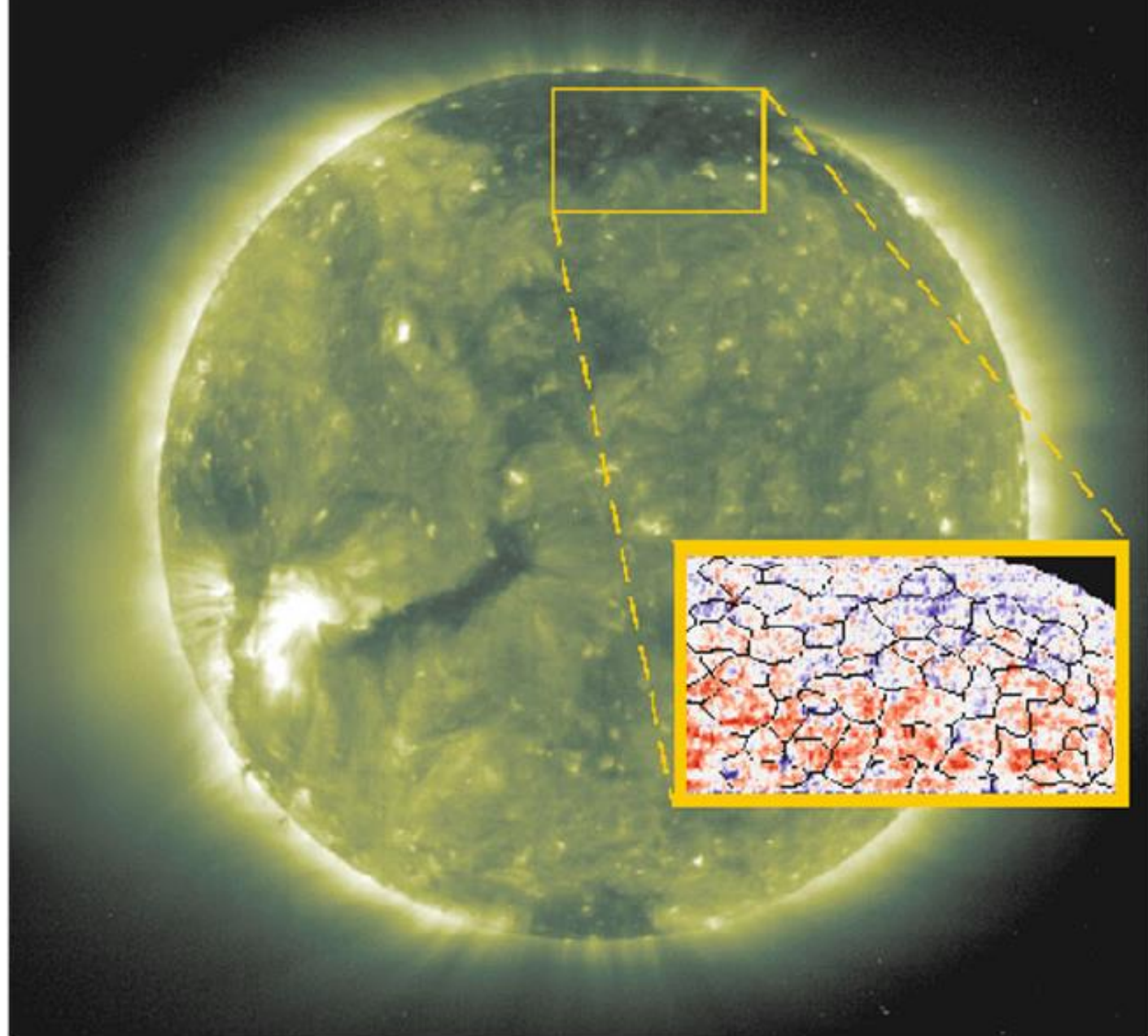
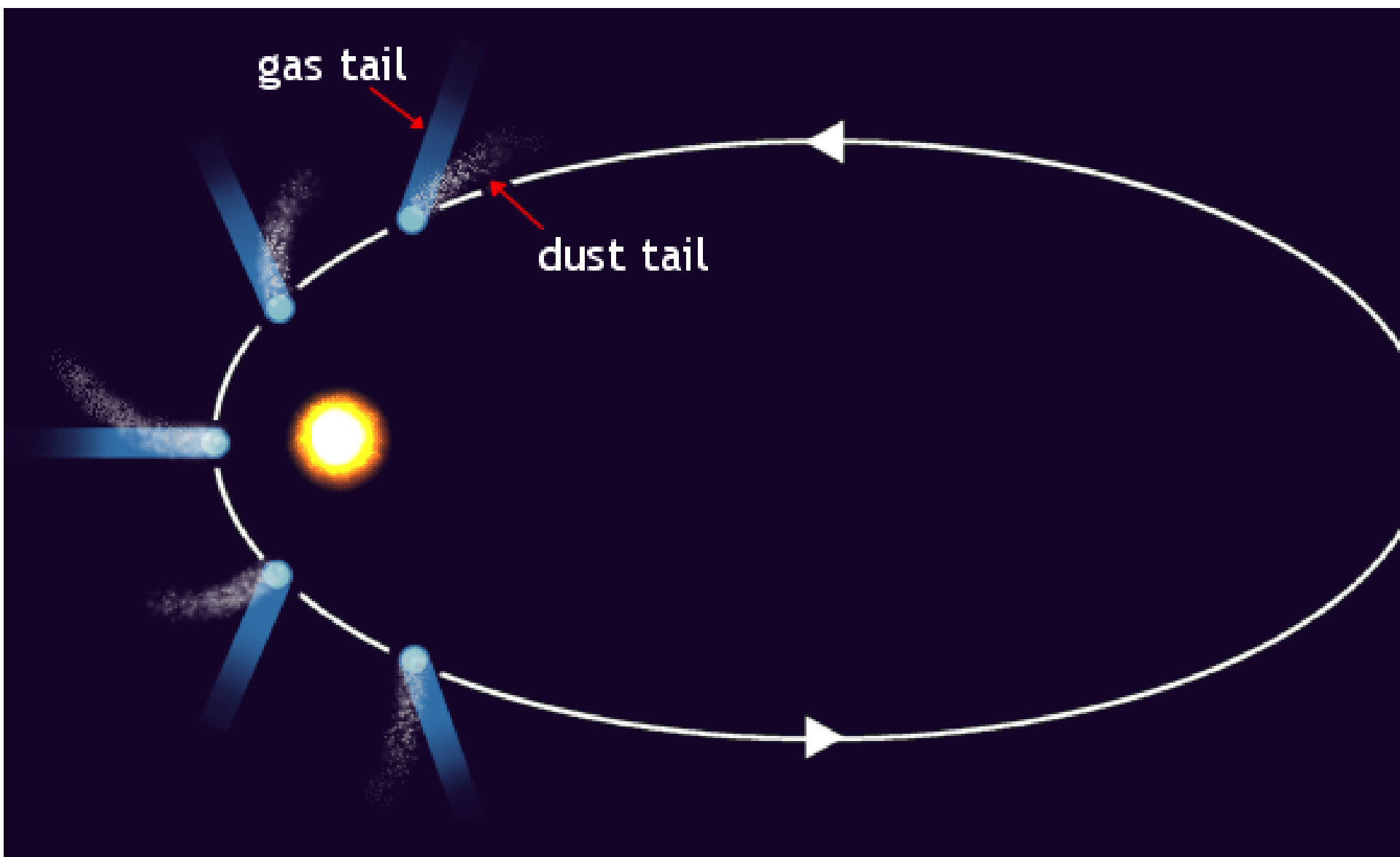


Fig. 9.12. The source region of the fast solar wind. This SOHO/EIT image in the

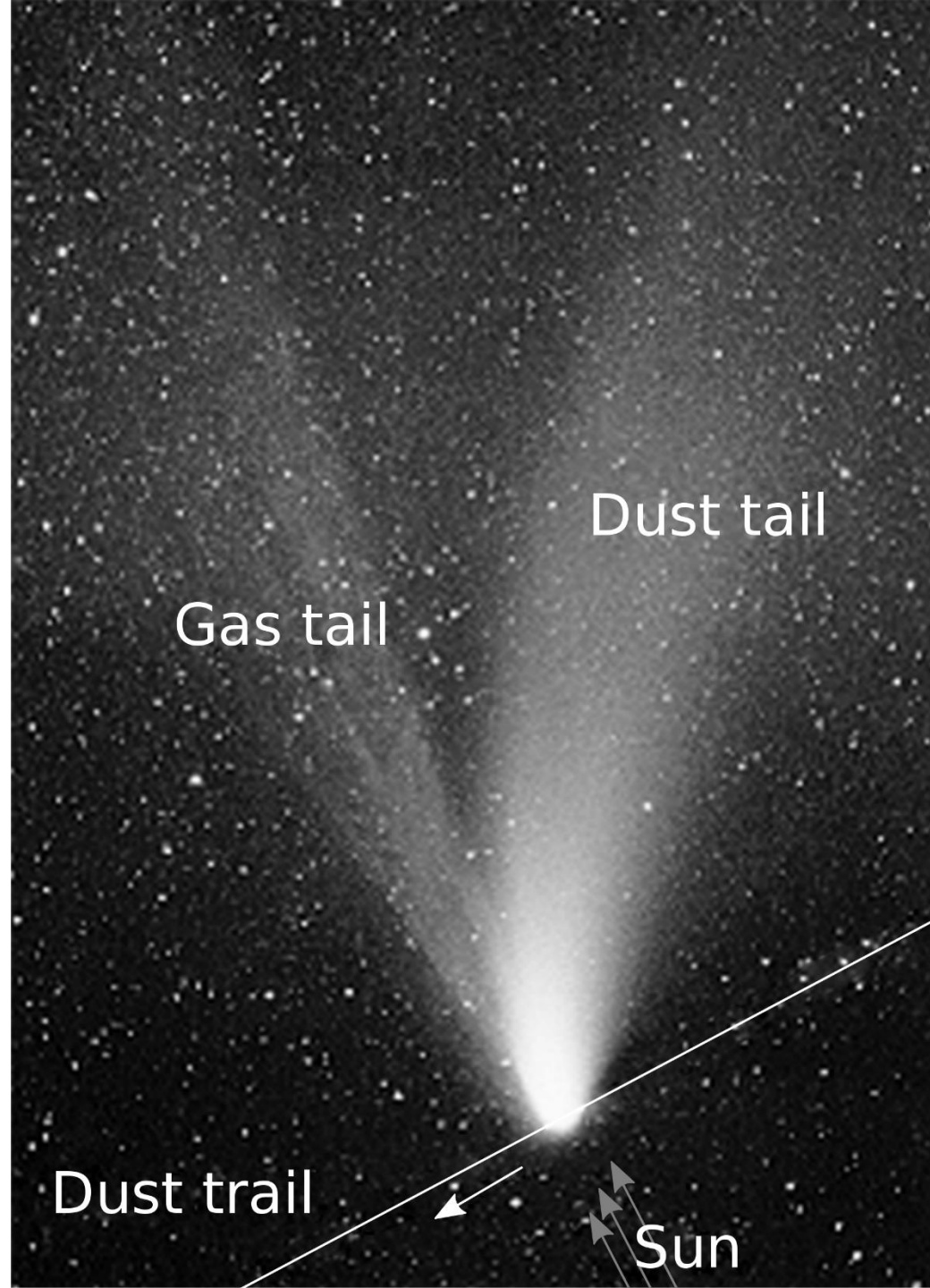






2 tails

- Gas tail ionized
 - Follows solar Wind
 - Dust tail trails behind
- Mariner II → direct evidence for wind
 - 400 km/s
- Apollo took samples
- Ulysses: high speed wind: 800 km/s



31 July 1995 - 15 December 1997

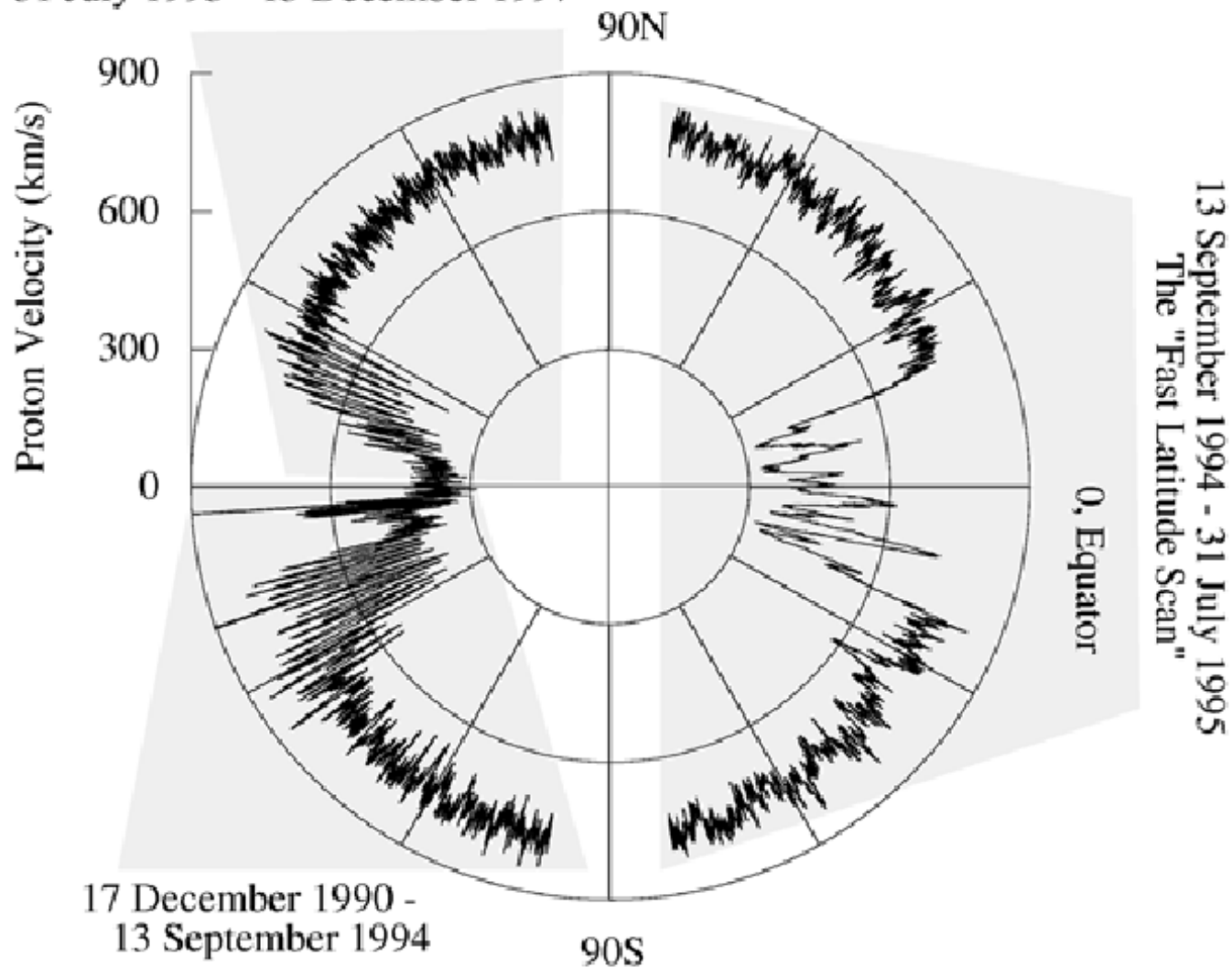


Fig. 9.13. Solar wind velocity versus heliographic latitude, measured by Ulysses

Properties

- Proton temperature 1.5×10^5 K
- Electron temperature 7.5×10^5 K
- Speed 400-800 km/s
- Mach number $u/c_s = 10-20$
- Alfvén Mach number $u/v_A = 5-10$
- Magnetic field 5 nT
- Fast wind from coronal holes



Next

664

(1 of 13)

Fit Page Width



Reload



Rotate Left



First Page

DYNAMICS OF THE INTERPLANETARY GAS AND MAGNETIC FIELDS*

E. N. PARKER

Enrico Fermi Institute for Nuclear Studies, University of Chicago

Received January 2, 1958

ABSTRACT

We consider the dynamical consequences of Biermann's suggestion that gas is often streaming outward in all directions from the sun with velocities of the order of 500–1500 km/sec. These velocities of 500 km/sec and more and the interplanetary densities of 500 ions/cm³ (10¹⁴ gm/sec mass loss from the sun) follow from the hydrodynamic equations for a 3×10^6 °K solar corona. It is suggested that the outward-streaming gas draws out the lines of force of the solar magnetic fields so that near the sun the field is very nearly in a radial direction. Plasma instabilities are expected to result in the thick shell of disordered field (10⁻⁵ gauss) inclosing the inner solar system, whose presence has already been inferred from cosmic-ray observations.

I. INTRODUCTION

Biermann (1951, 1952, 1957*a*) has pointed out that the observed motions of comet tails would seem to require gas streaming outward from the sun. He suggests that gas is often flowing radially outward in all directions from the sun with velocities ranging from 500 to 1500 km/sec; there is no indication that the gas ever has any inward motion. Biermann infers densities at the orbit of earth ranging from 500 hydrogen atoms/cm³ on magnetically quiet days to perhaps 10⁵/cm³ during geomagnetic storms (Unsöld and Chappuis 1949). The solar wind velocity is 10¹⁴–10¹⁵ gm/sec. It is the purpose of this

1	<input type="checkbox"/> 1958ApJ...128..664P Parker, E. N.	1665.000	11/1958	A	F G	R C
2	<input type="checkbox"/> 1979cmft.book.....P Parker, E. N.	1644.000	00/1979	A		C
3	<input type="checkbox"/> 1955ApJ...122..293P Parker, Eugene N.	1154.000	09/1955	A	F G	R C
4	<input type="checkbox"/> 1963idp..book.....P Parker, Eugene Newman	939.000	00/1963			C
5	<input type="checkbox"/> 1965P&SS...13....9P Parker, E. N.	921.000	01/1965	A	E	R C
6	<input type="checkbox"/> 1988ApJ...330..474P Parker, E. N.	916.000	07/1988	A	F G	R C
7	<input type="checkbox"/> 1957JGR....62..509P Parker, E. N.	768.000	12/1957		E	R C
8	<input type="checkbox"/> 1966ApJ...145..811P Parker, E. N.	679.000	09/1966	A	F G	R C
9	<input type="checkbox"/> 1972ApJ...174..499P Parker, E. N.	585.000	06/1972	A	F G	R C

 Find:
 Match case

Done

Assuming $c_s = 100 \text{ km/s}$, and using $G \approx 7 \times 10^{-11} \text{ m}^3 \text{ s}^{-2} \text{ kg}^{-1}$, $M = 2 \times 10^{30} \text{ kg}$, $1 \text{ AU} = 1.5 \times 10^{11} \text{ m}$, we have $r_* \approx 0.05 \text{ AU}$.

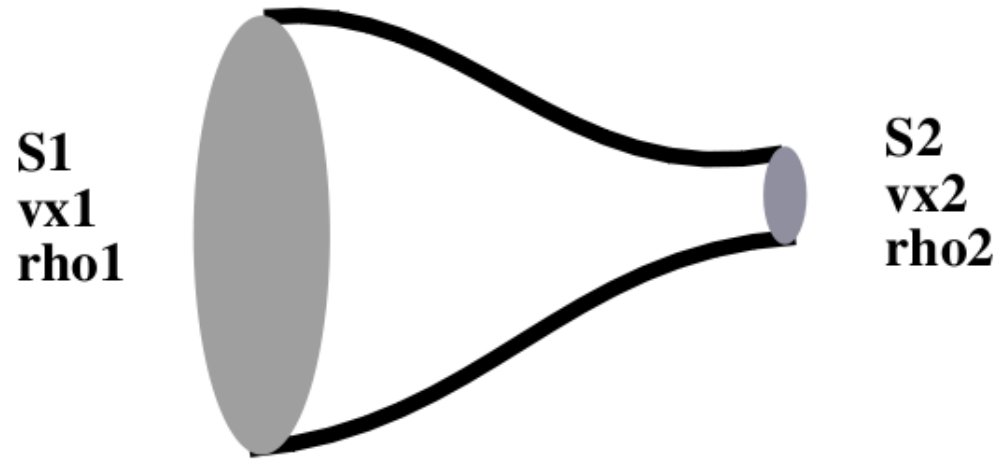


Figure 2.1: In the steady case we have $\nabla \cdot \rho \mathbf{v} = 0$. Using Gauss' divergence theorem it follows that $\oint \rho \mathbf{v} \cdot d\mathbf{S} = 0$. The two surfaces, S_1 and S_2 , are the only places where the $\mathbf{v} \cdot d\mathbf{S} \neq 0$.

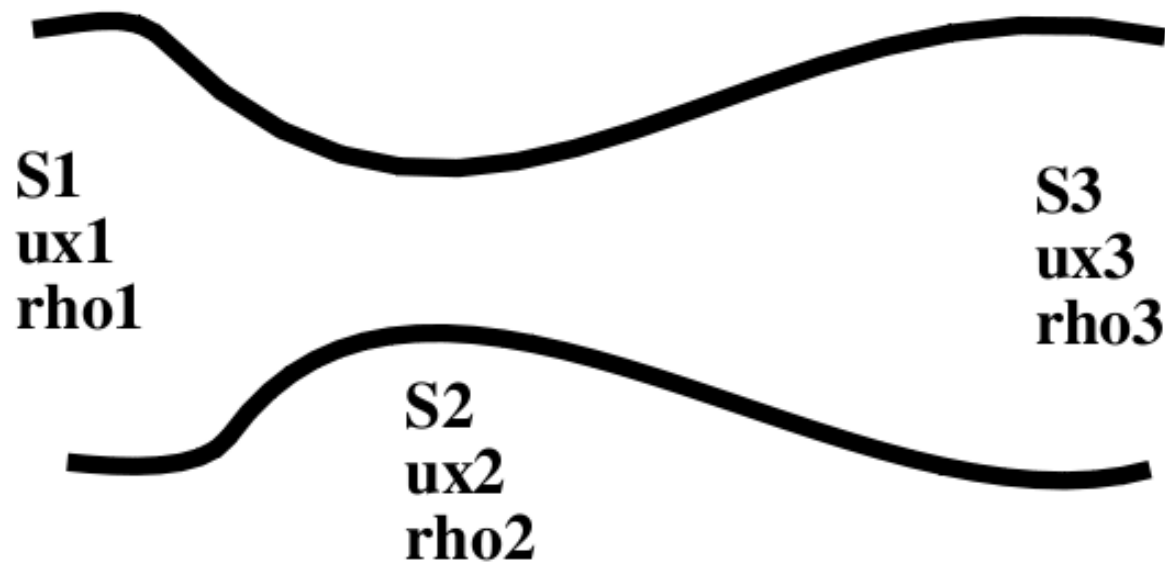


Figure 2.2: Cross-sectional area of a laval nozzle. If the flow is able to reach the sound speed at the point of minimal cross-section, it must go supersonic behind that point.

To find the energy for the critical solution we assume a critical radius r_* , so $c_s = \sqrt{GM/2r_*}$. At

Non-static corona

Continuity eqn

$$\frac{d}{dr} (r^2 \rho u_r) = 0$$

Momentum eqn

$$u_r \frac{du_r}{dr} = -c_s^2 \frac{d \ln \rho}{dr} - \frac{GM}{r^2}$$

isert

$$\left(u_r^2 - c_s^2\right) \frac{d \ln u_r}{dr} = \frac{2c_s^2}{r} - \frac{GM}{r^2}$$

Critical point

Logarithmic differentiation

Continuity eqn

$$\frac{d \ln r^2}{dr} + \frac{d \ln \rho}{dr} + \frac{d \ln u_r}{dr} = 0$$

Numerical solutions

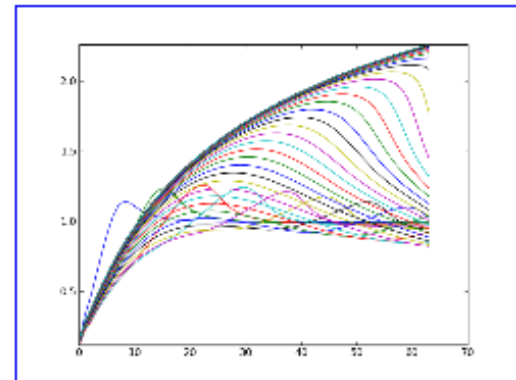
Parker Wind

→ Working material: [ParkerWind/](#), [ParkerWind.tar.gz](#) [untar this file by typing `tar xzf ParkerWind.tar.gz`]

The isothermal Parker wind is a solution of the equations

$$u \frac{du}{dr} = -cs^2 \frac{d \ln \rho}{dr} - \frac{GM}{r^2} \text{ and} \\ d(r^2 \rho u) / dr = 0$$

There is a critical point at $r = GM/2cs^2$. The numerical solution approaches the wind after some equilibration process. The initial condition was just $u_r = 1$.



What we learned today

- Corona: heating and wind acceleration
- Solar Wind
 - Smooth transition to supersonic
 - Critical point
 - Logarithmic differentiation